Available online at www.sciencedirect.com
ScienceDirect
Experimental Thermal and Fluid Science 32 (2008) 973–979
Experimental Thermal and Fluid Science
www.elsevier.com/locate/etfs

Studies of water level rise by entrained air in the surf zone

Ashabul Hoque *

Department of Mathematics, University of Rajshahi, Rajshahi 6205, Bangladesh

Received 11 January 2007; received in revised form 9 October 2007; accepted 15 November 2007

Abstract

This paper is concerned about the data analysis of void fractions in the surf zone measured by a conductivity probe. The experimental results show that void fraction distributions are the function of water depth and probe immersion time (duration of breaking event). Air volume of air bubbles calculated from void fraction data is found to be a function of shoreward distance. Moreover, this study focuses on the water level rise by entrained air would be a significant percent of wave set-up and scale effects occur in terms of air entrainment for $H_b < 0.30$ (m).

Keywords: Air–water measurements; Breaking waves; Surf zone; Air volume; Water level rise; Scale effect

1. Introduction

Wave breaking on beaches is a conspicuous, often impressive natural phenomenon. The surf zone is characterized by some air entrainments, which is highlighted by the "white waters". The sloping bottom affects the breaking process while a great amount of air bubble is entrained into water downstream of the breaking point. The sketch (Fig. 1) presents the cycle of air entrainment and detrainment process through a free surface at breaking waves. The characteristics of waves at breaking point in terms of breaking height and breaking depth have been analyzed thoroughly by many investigators over several decades [10,16].

Based on the evidence from the trial deployment and study from the relevant literature, bubble formation occurs before a wave breaks. During the wave breaks, an overturning jet is formed at the top of the wave crest. The jet is a feature common to both spilling and plunging breakers. Although air entrainment occurs both in spilling and plunging breaker, but plunging breakers have greater potential for air bubble entrainment [12,5]. Boundary between plunging and spilling waves is defined on the basis of Iribarren number I_0. The typical value in the range 0.45–3.2 suggests plunging waves, whereas spilling waves correspond to <0.45. The injected air bubbles beneath a breaking wave are rapidly broken up by turbulence, producing an initial size spectrum proportional to $(\text{radius})^{-10/3}$ [11]. This tiny air bubbles are not always visible to the naked eye, yet they play a very important role in the surf zone.

Although studies on surf zone air bubbles have been extensively studied in the past several years [1,9,14,17–19], its mechanism is not well understood, because, probably the flow fields of broken wave are very complicated after mixing the air bubbles. Air bubbles entrained by breaking waves play an important role in the transport of mass and energy across the air–sea interface [17]. Hoque and Aoki [14] reported that void fraction distribution is highly variable and in general the bubble density decreases with depth and increases with sea-state. Chanson et al. [2] found that the air entrainment process and bubble residence time are affected by the sloping bottom. Deane and Stokes [7] measured bubble size distributions inside the breaking waves in the laboratory and in the open ocean,

* Tel.: +880 721 750183; fax: +880 721 750064.
E-mail address: ashabulh@yahoo.com

0894-1777/$ - see front matter © 2007 Elsevier Inc. All rights reserved.
doi:10.1016/j.expthermflusci.2007.11.003

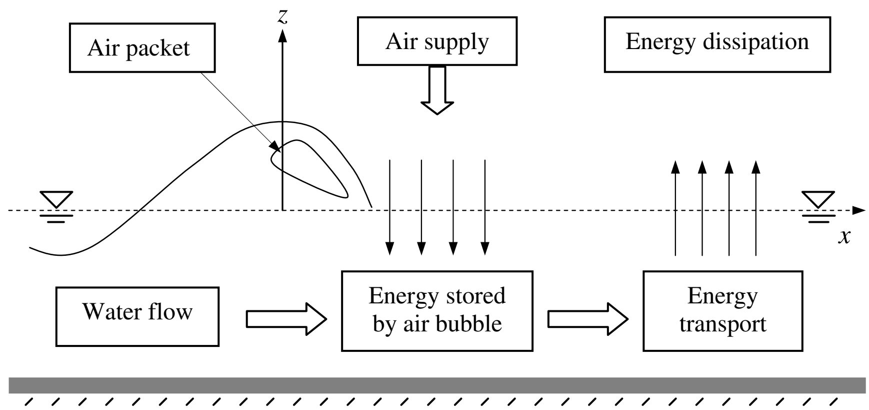

Fig. 1. Air entrainment and detrainment cycle.

provide a quantitative result for bubble formation in the laboratory. They also showed some images of bubbles and the evolving air–water mixture inside and beneath breaking wave crests and observed different air entrainment processes for different scales (Deane and Stokes [8]).

Air entrainment is associated with a rise in water level caused by liquid displacement upwards, which implies an increase in the potential energy [9]. Air bubbles entrained by breaking waves play an important role in the transport of mass and energy across the air–sea interface [17]. In this paper, we have described a device capable of measuring the void fraction data briefly and calculated air volume, energy dissipation and water level rise from measuring data. Moreover, this study focuses on the scale effects in terms of air entrainment in the surf zone.

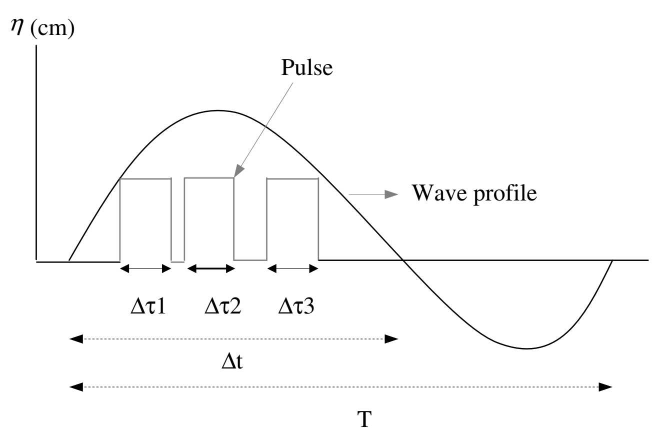

Fig. 2. A sketch of response of the wave gauge and probe.

Table 1
Wave breaking experiments: characteristics of wave breaking

Test (1)	H_0 (m) (2)	T (s) (3)	H_0/L_0 (4)	H_b (m) (5)	H_b/h_b (6)	I_0 (7)	Br. type (8)
SP-1	0.110		0.056	0.117	1.08	0.443	
SP-2	0.122	1.12	0.062	0.133	1.03	0.421	Spilling
SP-3	0.150		0.076	0.149	0.91	0.380	
PL-1	0.125		0.024	0.180	1.01	0.677	
PL-2	0.145	1.80	0.028	0.198	1.05	0.627	Plunging
PL-3	0.166		0.032	0.207	1.07	0.586	

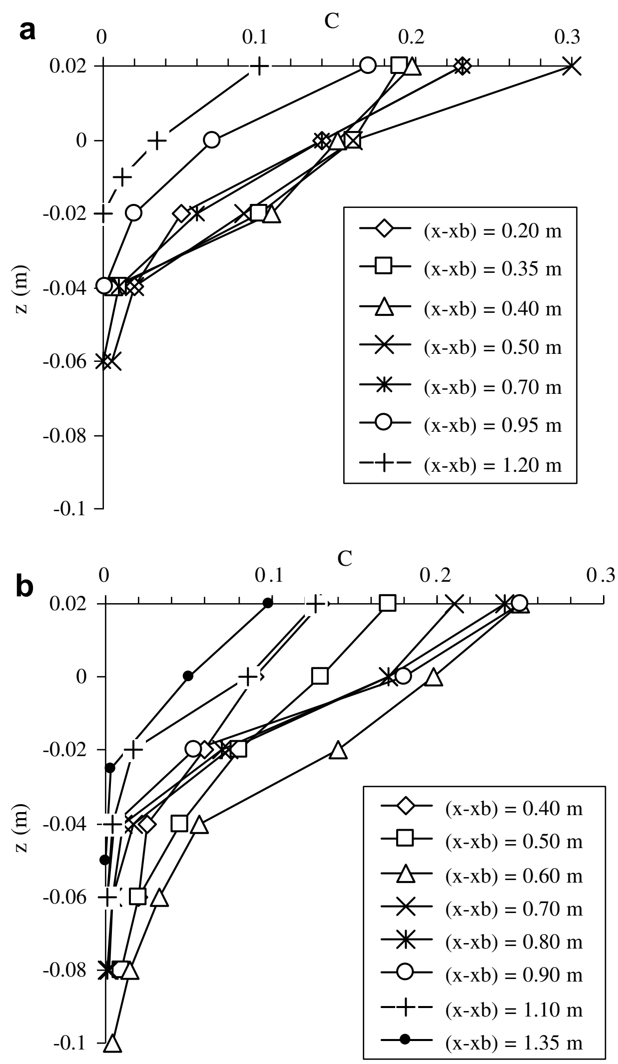

Fig. 3. Vertical distribution of mean void fraction during breaking event. (a) Spilling breaker ($H_0/L_0 = 0.076$) and (b) plunging breaker ($H_0/L_0 = 0.024$). Here x–x_b is the distance between wave breaking point and void fraction measuring point.

2. Experiments

2.1. Instrumentation

Two typical waves breaking were generated in a wave channel of 20 m long, 0.80 m wide, and 0.60 m deep. The bed slope of wave flume was 1/9.5. Experiments were conducted with tap water and ambient air. The effect of air bubbles on wave gauge and displacement meter reading was tested in preliminary experiments. Tests, performed with void fractions ranging from 0 to 0.10, showed that both wave gauges and displacement meter recorded with a reasonable accuracy the rise in water level induced by the air bubbles. The error was of the same order of magnitude as the bubble foam thickness formed at the water surface in the cylinder [14], Fig. 2.

The L-shape conductivity probe tip was set up in the opposite direction of wave propagation and void fraction was measured with a grid spacing of 5–25 cm increment along channel and 2 cm increment in the depth for two-dimensional wave breaking. Detailed measurements were performed for three tests in both cases of spilling and plunging breakers [13,14] and experimental conditions are tabulated in Table 1.

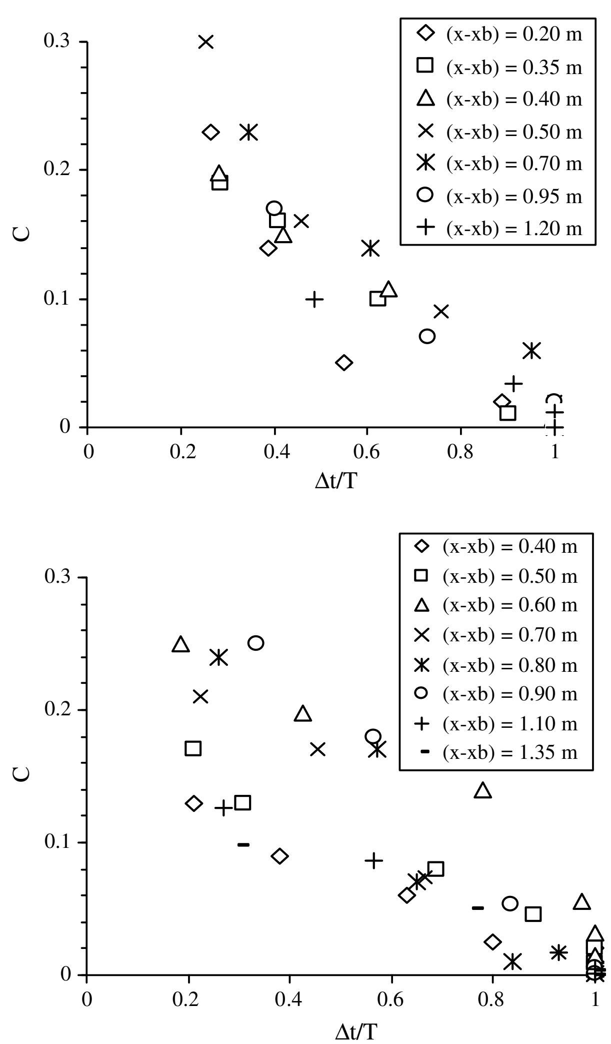

Fig. 4. Void fraction distribution as a function of dimensionless breaking duration time. (a) Spilling breaker ($H_0/L_0 = 0.076$) and (b) plunging breaker ($H_0/L_0 = 0.024$). Here $x - x_b$ is the distance between wave breaking point and void fraction measuring point.

2.2. Data processing

A sketch of air pulses and wave profile are shown in Fig. 2, which is used to determine the void fraction C. In data processing for the output from the wave gauges were multiplied by the calibration coefficient to obtain elevation of water. In the duration of breaking event which the probe is immersed under water, Δt, the total time of air bubble encounter, $\Delta\tau$, is given as

$$\Delta t = \sum_{\Delta t} \Delta\tau_i \tag{1}$$

where $\Delta\tau_i$ is the period that an air bubble takes when it passes the probe tip and i denotes number of air bubbles detected during Δt. The void fraction for one wave period T is obtained as

$$C = \frac{\sum_T \Delta\tau}{\sum_T \Delta t} \tag{2}$$

The above C represents the measurements of time averaged void-fraction during one wave period.

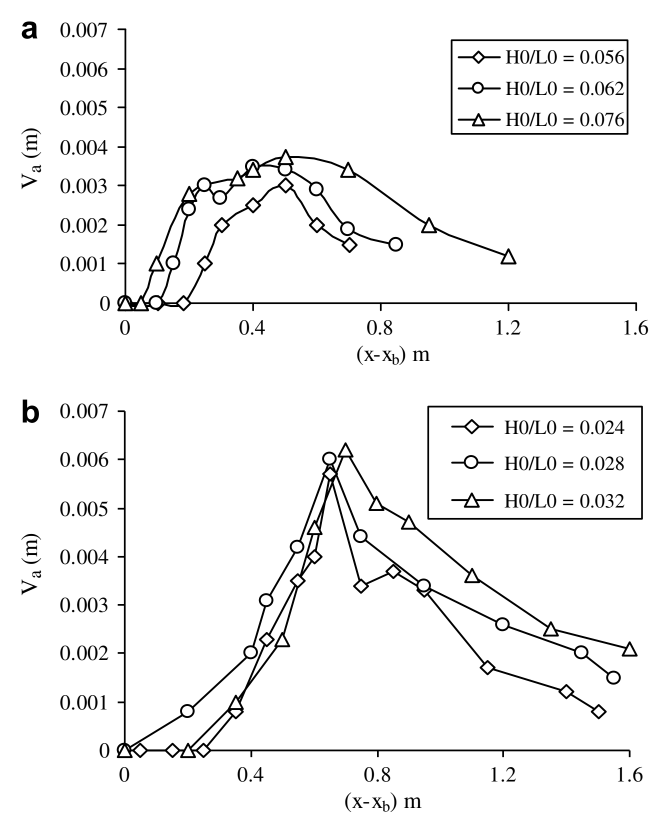

Fig. 5. Air volume distribution as a function of distance in the shoreward direction. (a) Spilling breaker and (b) plunging breaker.

3. Experimental results

3.1. Void fraction measurement

Air bubbles produced by breaking waves are measured in a laboratory tank by a conductivity probe under various wave conditions. Approximately 570 waves were extracted from 10 min data recording for each depth in spilling breaker, whereas it were 350–420 waves from 10 to 12 min data for plunging breaker. Finally, it was found that the mean void fraction C decreased exponentially for each vertical depth as shown in Fig. 3. The void fraction distributions followed closely analytical solutions of the air bubble diffusion equation [14].

Moreover, the relationship between the void fraction C and the time of immersion or the duration of breaking event, Δt at different elevations is illustrated in Fig. 4. Fig. 4(a) shows that void fraction decays linearly as the duration of breaking event increases, whereas the exponential relationship can be seen in several cases in Fig. 4(b). It could be urged that spilling and plunging breakers differ due to structure of turbulence. For the plunging breaker, the void fraction field is dominated by the turbulence more significantly than spilling breaker, especially near the free surface.

3.2. Volume of entrained air

The volume of entrained air, V_a, per unit length and width at each position within one wave period (time averaged air volume) were computed from the void fraction mappings (Fig. 3) using the following definition:

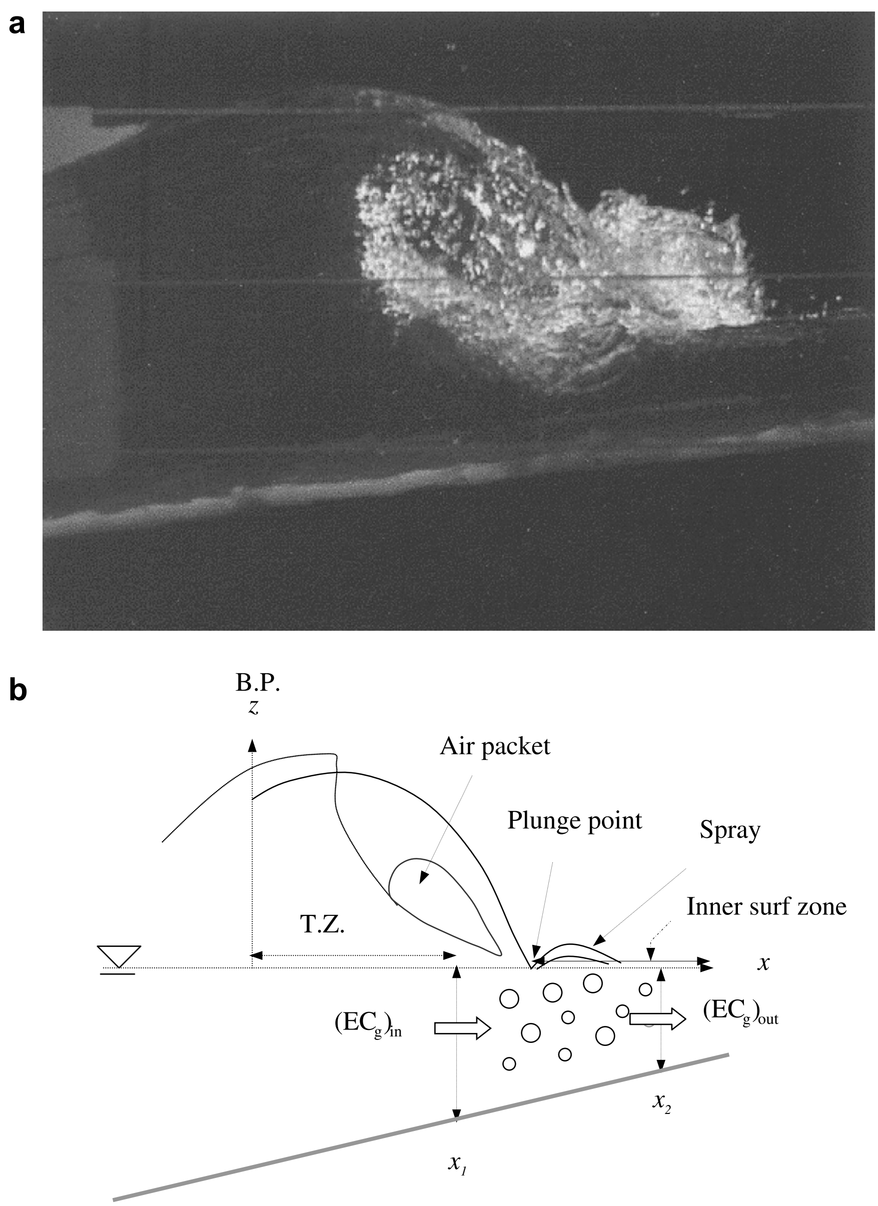

Fig. 6. Breaking waves. (a) Photograph and (b) sketch of a plunging breaker.

$$V_a = \int_{-h}^{\eta_+} C(z) * \frac{\Delta t(z)}{T} dz \tag{3}$$

where η_+ is the instantaneous water surface elevation.

Fig. 5 shows the variation of entrained air volume per unit area. From breaking point to a distance, the void fraction is almost zero, indicating no air entrained in the domain. It should be pointed out that the distribution of potential energy due to entrained air is found to be similar type configurations to air volume for vertical plunging jet (steady case), because it is proportional to entrained air volume [13]. In the surf zone (unsteady case), the entrained air volume is not only the function of depth, but also the duration of breaking event; the center-of-gravity of entrained air might be varied at each location. Fig. 5 shows that after transit zone to the position of maximum penetration (air bubble penetrated maximum at plunge point, see Fig. 6), V_a rapidly increases and subsequently decreases from plunging point to rest of inner zone.

3.3. Observed air volume

From video recordings of the 2-D breaking events from the side of the channel, the size of the "tube" of air initially enclosed by the plunging breakers was measured (Fig. 6(a)). In Fig. 6, the volume of air per unit width in the tube obtained from the video images, V_a^T, is plotted versus deep-water wave height. Fig. 7(a) suggests that volume of entrained air increases almost linearly as the wave height increases. Lamrre and Melville [17] observed that the volume of air enclosed in the initial air packet is conserved up to 1/4 of a wave period after breaking. However, the judgments of this issue may vary. It was also seen that the air packet was not created exactly from the breaking point (Fig. 6).

In Fig. 7(b) the energy dissipation by entrained air bubbles is plotted against the observed volume of air per unit width. The energy dissipation rate due to air bubbles in the wave breaking to the total energy dissipation rate D_a can be expressed as

$$D_a = \frac{E_{da}^T}{\Delta EC_g} \tag{4}$$

where E_{da} is the total energy dissipation by air bubbles and ΔEC_g is the total energy dissipation between local energy flux and the stable energy flux calculated from the following equations:

$$E_{da}^T = \rho_w g \int_{x_1}^{x_2} V_a w_r dx \tag{5}$$

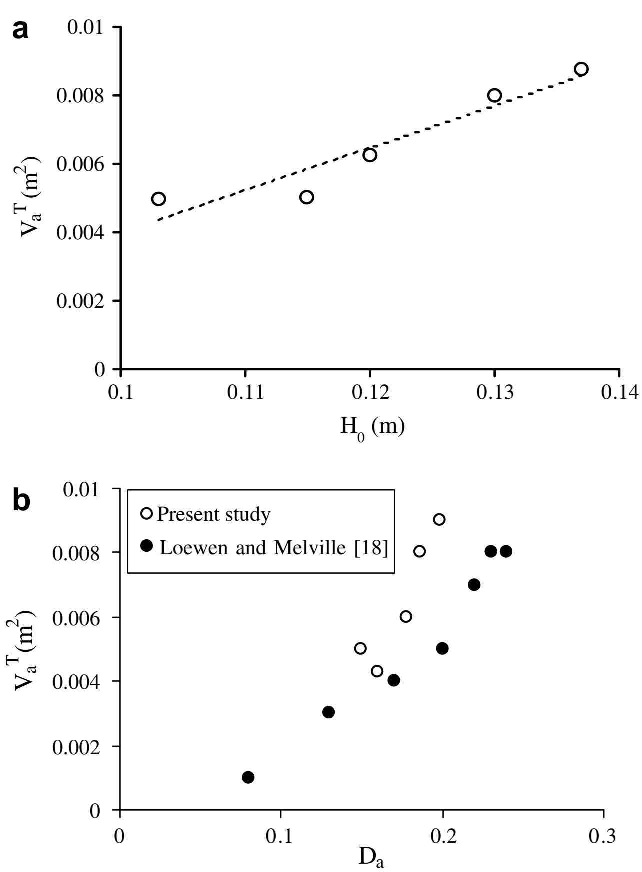

Fig. 7. Total volume of air in the tube formed by the plunging wave crest versus: (a) wave height and (b) energy dissipation rate.

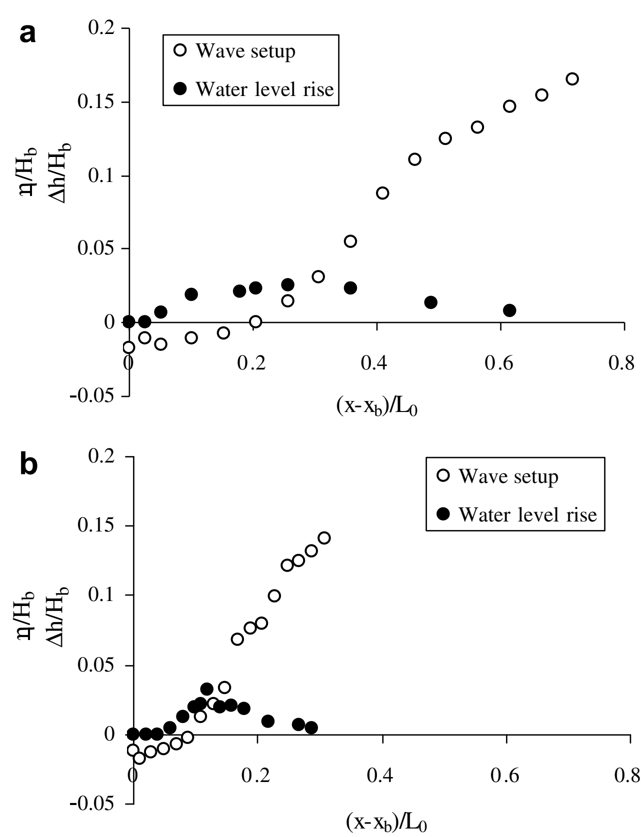

Fig. 8. Wave setup and estimated water level rise due to entrained air as a function of horizontal distance. (a) Spilling breaker ($H_0/L_0 = 0.076$) and (b) plunging breaker ($H_0/L_0 = 0.024$).

and

$$\Delta EC_g = \frac{1}{2}\rho_w g[\{a^2(gh)^{1/2}\}_{x_1} - \{a^2(gh)^{1/2}\}_{x_2}] \quad (6)$$

where x_1 and x_2 represent the offshore and onshore limits of aerated zone and ρ_w, a and h denote the water density, wave amplitude and water depth, respectively. The rise velocity w_r has been considered as 0.25 m/s [13].

Fig. 7(b) shows that the volume of air per unit width increases linearly as the energy dissipation increases. This relationship was first observed by Lamarre and Melville [17] who found that up to 50% of the energy dissipated by breaking was expended entraining air against the buoyancy force. In Fig. 7(b) correlation indicates that the amount of energy dissipated by breaking waves and the volume of entrained air is closely related. The data shows some discrepancies between present study and Loewen and Melville [18]. The reason of this may depend on the measurement technique, and this was very rough estimation. They measured the fractional energy dissipation, D_a using the following definition:

$$D_a = \frac{(\overline{\eta_0^2} - \overline{\eta_f^2})}{\overline{\eta_0^2}} \quad (7)$$

where $\overline{\eta_0^2}$ and $\overline{\eta_f^2}$ are the surface displacement variances upstream and downstream of the event, whereas in the present study, D_a has been measured by Eq. (4).

3.4. Water level rise

The contributions of waves and air bubbles are included in the data of wave set-up. From the experimental data, the effects of air bubble were exerted from wave set-up and plotted in Fig. 8. It was seen that a water level rise by air bubble would be a significant percent of wave set-up. Fig. 8 suggests that wave set-up occurs after a distance from breaking point where air bubbles appear. Interestingly, it has been seen that the contribution of air bubbles is almost zero in this domain (Fig. 6). This information is consistent with the suggestion reported by Dally et al. [6]. Their suggestion was that no energy is dissipated until the curl touches down and "white water" appears (Fig. 6(a)).

We have also compared the data of water level rise by entrained air bubbles with that of Hwung et al. [15] in Fig. 9 for both of plunging and spilling breakers. The data of water level rise was exerted from potential energy of air bubbles in the case of Hwung et al. [15]. A similar trend in the distribution of water level rise due to air bubbles is observed although the shoreward distances $(x-x_b)/L_0$ are not same. Fig. 9 shows that water level rise due to entrained air in plunging breaker is greater than that in spilling breaker. In Fig. 9, the results observe that there are significant discrepancies between present study and Hwung et al. [15]. The reason of this may be the bottom slope. Because in the present study the bottom slope was a little bit steeper than Hwung et al. [15] which may produce the breaking process in the short way, i.e, if the bottom slope is mild then wave breaking process continue in a long period, results in air entrainment process also continue.

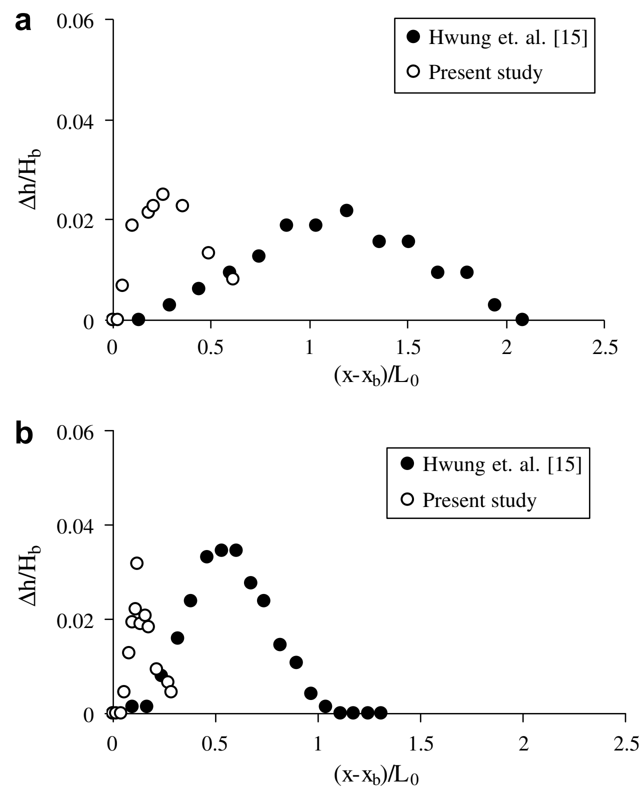

Fig. 9. Comparisons the non-dimensional water level rise. (a) Spilling breaker and (b) plunging breaker.

3.5. Scale effect

We studied the effects of air entrainment at vertical circular plunging jets in laboratory experiment and found a significant scale effect when $We_1 < 1000$ [10]. Applying this value the scale effects can be discussed for plunging breaking waves.

At plunging breakers, the jet impact velocity V_1 and water jet thickness d_1 may be roughly estimated as $\sqrt{2gH_b}$ and $0.05H_b$, respectively, where H_b is the wave height at breaking point [3]. For example, $V_1 = \sqrt{2gH_b}$ (m/s), $d_1 = 0.05$ H_b (m), $\rho_w = 1000$ (kg/m^3), $\sigma = 0.073$ (N/m), and with the consideration of 1000 for critical Weber number $We_1 = \rho_w V_1^2 d_1/\sigma$, this gives about 0.30 (m) for H_b. Larger and smaller values of H_b are possible for different consideration of We_1, but scale effects occur for $We_1 < 1000$. This yields scale effects, which may be significant in the laboratory for $H_b < 0.30$ (m).

Similar conclusion was made by Chanson et al. [4] and Hall [12]. They noted that entrained air bubbles would not be similar in small-scale physical models because of lack of similarity of the Weber number between field and laboratory.

4. Conclusions

Air entrainment in the surf zone was investigated for a range of flow conditions (Table 1). The experimental results showed that the void fraction decreased with increasing both the water depth and the duration of breaking event. Air volume calculated from void fraction data was found to be a function of shoreward distance. Moreover, visual observations suggested that the volume of air in the tube was increased almost linearly with the wave height and the energy dissipation rate (D_a).

The results demonstrated that the contribution in raising the water level due to entrained air on wave set-up was found a significant percent. Moreover, laboratory studies of breaking waves may be affected by scale effects in terms air entrainment for $H_b < 0.30$ (m).

Acknowledgement

The author thanks Dr. Roushown Ali, Dr. G. C. Paul and three referees for their valuable suggestions.

References

[1] H. Chanson, Air–water and momentum exchanges in unsteady surging waters: an experimental study, Exp. Therm. Fluid Sci. 30 (2005) 37–47.
[2] H. Chanson, S. Aoki, M. Maruyama, Unsteady air bubble entrainment and detrainment at a plunging breaker: dominant time scales and similarity of water level variations, Coastal Eng. 46 (2002) 139–157.
[3] H. Chanson, J.F. Lee, Plunging jet characteristics of plunging breakers, Coastal Eng. 31 (1997) 125–141.
[4] H. Chanson, S. Aoki, A. Hoque, Bubble entrainment and dispersion in plunging jet flows: freshwater vs. seawater, J. Coastal Res. 22 (3) (2006) 664–677.
[5] E.D. Cokelet, Breaking waves, Nature 267 (1977) 769–774.
[6] W.R. Dally, R.G. Dean, R.A. Dalrymple, Wave height variation across beaches of arbitrary profile, J. Geophys. Res. 90 (C6) (1985) 11917–11927.
[7] G.B. Deane, M.B. Stokes, Scale dependence of bubble creation mechanisms in breaking waves, Nature 416 (2002) 839–844.
[8] G.B. Deane, M.B. Stokes, Air entrainment processes and bubble size distributions in the surf zone, J. Phys. Oceanogr. 29 (1999) 1393–1403.
[9] A. Führböter, Air entrainment and energy dissipation in breakers, Proc. ICCE (1970) 391–398.
[10] C.J. Galvin, Breaker type classification on three laboratory beaches, J. Geophys. Res. 73 (12) (1968) 3651–3659.
[11] C. Garrett, M. Li, D. Farmer, The connection between bubble size spectra and energy dissipation rates in the upper ocean, J. Phys. Oceanogr. 30 (2000) 2163–2171.
[12] K.R. Hall, Aeration in rubble-mound breakwater models, J. Water Port Coastal Ocean Eng. ASCE 116 (1990) 400–405.
[13] A. Hoque, Air bubble entrainment by breaking waves and associated energy dissipation, Ph.D. thesis, TUT, Japan, 2002, 151 p.
[14] A. Hoque, S. Aoki, Distribution of void fraction under breaking waves in the surf zone, Ocean Eng. 32 (2005) 1829–1840.
[15] H. Hwung, J. Chyan, Y. Chung, Energy dissipation and air bubbles mixing inside surf zone. in: Proc. 23rd ICCE, ASCE, 1992, pp. 308–321.
[16] C. R. Iribarren, C. Nogales, Protection des ports. Section II, Comm. 4, XVIIth Int. Nav. Congress, Lisbon, 1949.
[17] E. Lamarre, W.K. Melville, Air entrainment and dissipation in breaking waves, Nature 351 (1991) 469–472.
[18] M.R. Loewen, W.K. Melville, An experimental investigations of the oscillations of bubble plumes entrained by breaking waves, J. Acoust. Soc. 96 (3) (1994) 1329–1343.
[19] J. Wu, Bubbles in the near-surface ocean: a general description, J. Geophys. Res. 93 (1988) 587–590.